Mon. Not. R. Astron. Soc. **328,** 805–809 (2001)

The 2dF QSO Redshift Survey – VIII. Absorption systems in the 10k catalogue

P. J. Outram,[1★] R. J. Smith,[2,3] T. Shanks,[1] B. J. Boyle,[4] S. M. Croom,[4] N. S. Loaring[5] and L. Miller[5]

[1]*Department of Physics, University of Durham, South Road, Durham DH1 3LE*
[2]*Astrophysics Research Institute, Liverpool John Moores University, 12 Quays House, Egerton Wharf, Birkenhead CH41 1LD*
[3]*Research School of Astronomy & Astrophysics, Mount Stromlo Observatory, Institute of Advanced Studies, Australian National University, Private Bag, Weston Creek PO, ACT 2611, Australia*
[4]*Anglo-Australian Observatory, PO Box 296, Epping, NSW 2121, Australia*
[5]*Department of Physics, University of Oxford, Nuclear & Astrophysics Laboratory, Keble Road, Oxford OX1 3RH*

Accepted 2001 August 10. Received 2001 July 30

ABSTRACT

We examine the highest signal-to-noise ratio spectra from the 2dF QSO Redshift Survey (2QZ) 10k release and identify over 100 new low-ionization heavy-element absorbers: damped Lyman α (DLA) candidates suitable for higher-resolution follow-up observations. These absorption systems map the spatial distribution of high-z metals *in exactly the same volumes* as the foreground 2QZ QSOs themselves sample and hence the 2QZ gives us the unique opportunity to compare directly the two tracers of large-scale structure. We examine the cross-correlation of the two populations to see how they are relatively clustered, and, by considering the colour of the QSOs, detect a small amount of dust in these metal systems.

Key words: surveys – quasars: absorption lines – cosmology: observations – large-scale structure of Universe.

1 INTRODUCTION

Progress in the study of quasi-stellar object (QSO) absorption-line systems has gone hand in hand with the advancement of technology over the past few years. During the 1980s developments in echelle spectroscopy with sensitive electronic detectors increased the attainable resolution by a factor of 10. The detailed analysis of the absorption systems in these spectra was possible through absorption-line profile fitting. The increase in spectral dispersion coupled with the need to obtain a respectable signal-to-noise (S/N) ratio, however, forced astronomers to observe the same object for many nights on 4-m-class telescopes, restricting the number of objects it was possible to observe. In the 1990s the 10-m Keck telescope together with its powerful instrument HIRES enabled us to obtain optical spectra of faint, high-redshift QSOs at unprecedented spectral resolution ($\sim 7\,\mathrm{km\,s^{-1}}$) and a signal-to-noise ratio in excess of 100 in a single night. Meanwhile, ultraviolet spectroscopy using the *Hubble Space Telescope* (*HST*) opened a window on QSO absorbers at low redshift. Using these data, very detailed studies of the chemical properties of the largest absorbers, damped Lyman α systems (DLAs), have provided a wealth of information concerning the formation of structure. Understanding the chemical evolutionary history of galaxies, seen here in absorption, is fundamental to the study of galaxy formation.

The study of DLAs has suffered from the small number of objects, approximately 100, that are currently known. Although detailed studies of individual objects are very revealing, *HST* imaging of QSO fields has revealed a wide range of luminosities and morphologies for DLA counterparts. Hence to determine the evolution in the absorption properties of a such mixed population of galaxies, much larger samples of QSO absorbers will be required.

With the recent release of the 2dF QSO Redshift Survey (2QZ) 10k catalogue (Croom et al. 2001a) the number of known QSOs has suddenly and dramatically increased. With the 2QZ rapidly approaching its target of 25 000 QSOs, together with the Sloan Digital Sky Survey observations (Fan et al. 1999), unprecedented numbers of new QSO spectra will soon be available from which we can identify and study large numbers of new heavy-element absorption systems.

As the 2QZ spectra were taken primarily to confirm the identity of QSOs, and determine their redshift, they have a typical S/N ratio ~ 10, and a resolution of ~ 8 Å. Although this is not ideal for absorption-line analysis, it is possible to identify strong heavy-element absorption systems, especially those with distinctive features, such as Mg II/Fe II absorption.

In this paper we examine the highest S/N ratio spectra from the

★E-mail: Phil.Outram@durham.ac.uk

2QZ 10k release and identify over 100 new heavy-element absorbers, suitable for higher-resolution follow-up. These absorption systems map the spatial distribution of high-z gas and metals *in exactly the same volumes* as the foreground 2QZ QSOs themselves sample and hence the 2QZ gives us the unique opportunity to directly compare the two tracers of large-scale structure. We examine the cross-correlation of the two populations to see how they are relatively clustered. Finally, we consider the colour of the QSOs containing absorption systems, relative to the 2QZ average and detect a small amount of dust in these metal systems.

2 2QZ SPECTRA

The 2QZ comprises two $5 \times 75\,\mathrm{deg}^2$ declination strips, one at the South Galactic Pole and one in an equatorial region in the North Galactic Cap. QSOs candidates were selected by ultraviolet excess (UVX) in the U–B : B–R plane, using automated plate measurements (APM) of UK Schmidt Telescope photographic plates (Smith et al. 2001).

2QZ objects were observed with the 2° field instrument (Lewis, Glazebrook & Taylor 1998) on the Anglo-Australian Telescope (AAT) using the low-resolution 300B grating, providing a dispersion of $178.8\,\text{Å}\,\mathrm{mm}^{-1}$ ($4.3\,\text{Å}\,\mathrm{pixel}^{-1}$) and a resolution of ~ 8.6 Å($\sim$2 pixels) over the wavelength range 3700–7500Å. Each field received approximately 1-h integration, adjusted to match conditions where possible.

The data were reduced using the pipeline reduction system 2DFDR (Bailey & Glazebrook 1999). Following bias subtraction, the spectra from each fibre were extracted and wavelength calibrated using a CuAr + He arc. Sky subtraction was done using a mean sky spectrum determined from between 6 and 20 sky-dedicated fibres in each frame.

The reduced 2dF spectra were identified automatically by AUTOZ (Miller et al., in preparation), which also determines the redshift of the QSOs. These identifications were confirmed by eye. Approximately 18 000 QSO redshifts have been obtained to date, making this survey already an order of magnitude larger than any previous QSO survey.

The primary science goal of the 2QZ is to obtain an accurate measure of large-scale structure via the study of QSO clustering. The observations are therefore optimized to maximize the number of QSO identifications. Hence the S/N ratio and resolution, whilst ideal for identifying broad emission features, are generally too low to detect all but the strongest narrow absorption features. Furthermore, the sky-subtraction possible on a multifibre instrument such as 2dF is relatively poor, leading to large uncertainties in the zero-level of the spectra (making equivalent width measurements less reliable), and variable sky lines, particularly at the red end of the spectrum. Having said that, the 10 000 QSO spectra released so far are still, as we shall demonstrate, a hugely valuable resource for QSO absorption-line studies.

3 ABSORPTION SYSTEMS

To detect absorption systems in the spectra of the 2QZ QSOs released in the 10k catalogue (Croom et al. 2001a), QSOs with $z_{\mathrm{abs}} > 0.5$ and S/N ratio > 15 were selected from the catalogue for examination by eye. Systems identified by two or more absorption features are included in this analysis (owing to the resolution of the spectra, doublets such as C IV $\lambda\lambda$1548,1550 and Mg II $\lambda\lambda$2796,2803 were counted as single features). As the primary aim of this paper is to identify heavy-element systems that could correspond to DLA candidates, only systems that exhibit low ionization absorption features are reported here. Several of the spectra examined were BAL QSOs, or exhibited relatively high ionization $z_{\mathrm{abs}} \sim z_{\mathrm{em}}$ systems, which are excluded from this analysis. Also excluded were several C IV systems, often with associated Si IV and H I absorption. Finally, all unconfirmed single-absorption features are excluded, including Lyα absorbers in the forest of high-redshift QSOs that do not exhibit metal features, and individual metal features that most likely correspond to C IV or Mg II systems.

In total, 137 low-ionization absorption systems were detected in 1266 QSO spectra. Of these, 120 are Mg II systems, and the remaining 17 are C IV systems at higher redshift, which also exhibit low-ionization species, and in 12 cases, strong Lyα absorption. Of these, two have a rest equivalent width in excess of 10 Å, and hence are strongly damped Lyα line candidates. Three example 2QZ spectra showing absorption systems are shown in Fig. 1, and Table 1 contains a full list of the low-ionization absorption systems. Where possible the rest equivalent width (W_0) of the Mg II $\lambda\lambda$2796,2803 doublet (Å), or H I λ1215 for the high-redshift systems, is quoted. Owing to the low resolution of the data the separate Mg II features are often not resolved. The W_0 determination is not highly reliable owing to the relatively poor sky subtraction possible with fibre observations, leading to zero-level uncertainty, particularly at the blue end of the spectrum. Also, there is relatively high continuum uncertainty owing to the low S/N ratio and resolution of the data, particularly in the Lyα forest. Typical uncertainty in the W_0 is of the order of 20 per cent.

4 QSO ABSORBERS AND LARGE-SCALE STRUCTURE

The largest heavy-element absorption systems, DLAs, are generally believed to be the progenitors of present-day spiral galaxies (Wolfe 1995). They dominate the mass of neutral gas at redshift $z \simeq 3$, a mass comparable with that of the stars in present-day spiral discs, suggesting that DLAs are the source of most of material available for star formation at high redshift (Lanzetta, Wolfe & Turnshek 1995). 21-cm emission surveys of the local universe have found that the contribution from intergalactic gas to the H I cross-section is negligible, whereas spirals contribute around 90 per cent (Rao & Briggs 1993), adding further weight to this hypothesis. *HST* imaging of QSO fields has been carried out in an attempt to determine the morphology and size of DLA absorbers. A wide range of luminosities and morphologies were seen, a result inconsistent with the standard H I disc paradigm (Le Brun et al. 1997; Rao & Turnshek 1998). Pettini et al. (1999) showed, furthermore, that the metallicity of DLAs does not increase towards solar values with decreasing redshift, as expected by the large spiral progenitor model, but instead little evolution is seen, with metallicities staying subsolar. It is possible that dust in the most metal-rich galaxies obscures light from any background QSO, making these objects too faint to see (Pei & Fall 1995). If so, this dust bias could help explain why the observed DLAs appear metal poor in comparison to present-day galaxies. Another possible explanation is that the absorption cross-section may be dominated by diffuse objects with relatively low star formation rates, whereas rapid star formation occurs in the most compact galaxies (Mo, Mao & White 1999). This evidence all points towards a mixed population of galaxies, with a large fraction of low-mass, or perhaps low surface brightness galaxies, being

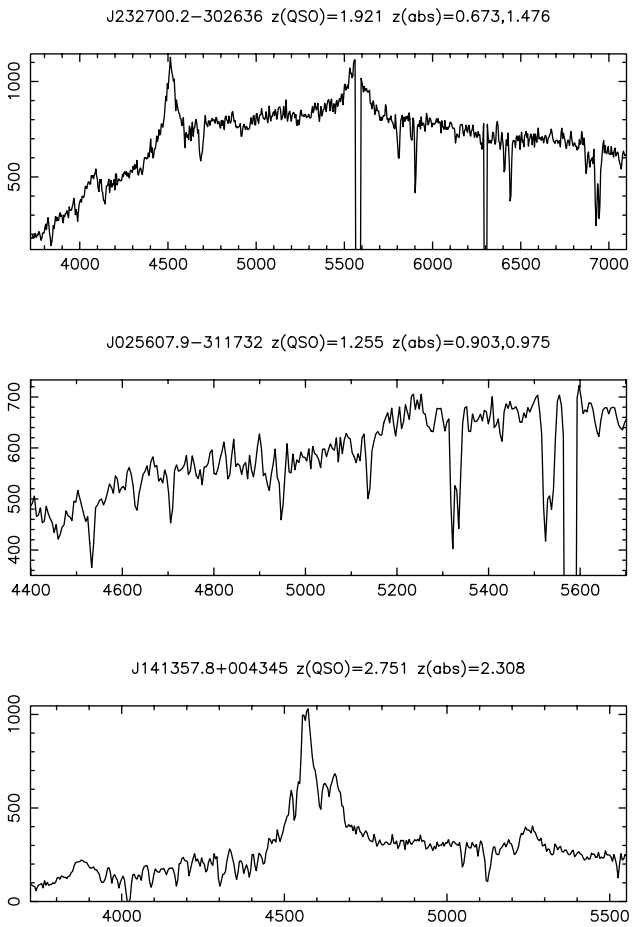

Figure 1. Examples of 2QZ spectra containing identified absorption systems. The first spectrum shows the distinctive pattern of Fe II absorption at 5850 and 6420 Å, Mg I at 7060 Å and the strong Mg II doublet at 6930 Å, together with C IV absorption 3830 Å, Al II at 4140 Å, and Si II at 3780 Å all owing to a system at $z_{\rm abs} = 1.476$. A second system lies at lower redshift; the Mg II doublet at 4680 Å is visible, along with Fe II absorption at 3980 Å, and 4350 Å. Two further examples of Mg/Fe systems can be seen in the second spectrum. The final spectrum has a distinctive Lyα forest. The H I λ1215 line at 4020 Å is a strong DLA candidate with corresponding C IV absorption at 5120 Å, Al II at 5525 Å, and Si II at 5050 Å amongst the other ions visible.

responsible for the DLA absorbers, rather than the simpler spiral progenitor model (Vladilo 1999).

QSO imaging experiments at redshifts out to $z \sim 2$ suggest that the clustering environment of UVX QSOs is similar to optically selected galaxies (Smith, Boyle & Maddox 1995; Croom & Shanks 1999). By measuring the two-point autocorrelation function of the 2QZ QSOs, Croom et al. (2001b) compared the clustering of QSOs at redshift $\bar{z} \sim 1.4$ with the clustering of normal galaxies locally ($\bar{z} \sim 0.05$) and concluded that the clustering properties are very similar. It would be preferable, however, to compare directly the clustering of QSOs and galaxies in the same redshift intervals. Whilst determining accurate redshifts for a large sample of high-redshift optically selected galaxies is challenging, absorption-line analysis offers a complementary approach to constraining the QSO–galaxy bias.

To examine how the absorption systems cluster relative to the 2QZ QSOs, we calculate the two-point absorber–QSO cross-correlation function, $\xi_{\rm AQ}(s)$, in an $\Omega_{\rm m} = 0.3$, $\Omega_\Lambda = 0.7$ cosmology. To estimate the effective volume of each bin, a catalogue of unclustered, random points that have the same radial selection function and angular mask, and approximately 20 times the mean density as the 2QZ QSOs is constructed, taking into account Galactic extinction (Schlegel, Finkbeiner & Davis 1998). The random catalogue number density is normalized to the number of observed QSOs on each UK Schmidt Telescope (UKST) plate to correct for possible small residual calibration errors in the relative magnitude zero points of the UKST plates (see Croom et al. 2001b for further details). We use the estimator

$$\xi_{\rm AQ}(s) = \frac{D_{\rm abs}D_{\rm QSO}(s)\bar{n}_R}{D_{\rm abs}R_{\rm QSO}(s)\bar{n}_{\rm QSO}},$$

where $D_{\rm abs}D_{\rm QSO}(s)$ is the number of absorber–QSO pairs at a given separation in redshift space, s, and $D_{\rm abs}R_{\rm QSO}(s)$ is the number of absorber–random pairs. As we are determining the average clustering of QSOs about each absorber, the spatial distribution of the absorbers themselves is not important (this distribution is not straightforward as the absorbers are selected along multiple lines of sight through the volume). The errors are calculated using the Poisson estimate, which is accurate at small scales, $< 50\,h^{-1}$ Mpc, because each pair is independent. All absorbers that lie within $\delta z = 0.05$ of the emission redshift of the QSO are excluded from the analysis to ensure that we are only considering truly intervening absorbers. In fact, all of the absorber–QSO pairs within $100\,h^{-1}$ Mpc separation are caused by an absorber in a different line of sight to the QSO.

The absorber–QSO cross-correlation function, $\xi_{\rm AQ}(s)$, is shown in Fig. 2. As there are relatively few absorbers in the analysis, the errors are still quite large and clustering is only detected at the 1.5σ level. The amplitude of the clustering appears to agree remarkably well with the QSO autocorrelation measurement (Croom et al. 2001b); further evidence that QSOs are clustered like normal galaxies at these high redshifts. By including absorption systems detected in low S/N ratio spectra, and extending this analysis to the full 2QZ data set when the survey is complete it will soon be possible to measure the cross-correlation function to much higher precision.

5 QSO COLOUR AND DUST IMPLICATIONS

The average colour of the QSOs in this sample is $(\overline{B_J - R})_{\rm abs} = 0.546$. To test whether the QSO spectra have been reddened by dust in the foreground absorption systems, we compare this colour with the average colour of QSOs in the 2QZ catalogue. As QSO colour is redshift dependent, we draw random samples from the full catalogue with the same redshift distribution as the QSOs in this absorption-line sample to produce a fair comparison. The resultant expected QSO colour for a random sample of 2QZ QSOs of this size and redshift distribution is $(\overline{B_J - R})_{\rm QSO} = 0.493 \pm 0.026$. Hence we have a 2σ detection of reddening in the absorption system QSOs. The spectra are reddened by an average of $E(B_J - R) = 0.053$, corresponding to a visual extinction $A(V) = 0.13$, assuming an $R_V = 3.1$ extinction curve (Schlegel et al. 1998).

Adopting the relationship between interstellar extinction and neutral hydrogen gas column density from Bohlin, Savage & Drake (1978),

$$\langle N({\rm H\,I} + {\rm H_2})/E(B-V)\rangle = 5.8 \times 10^{21}\,{\rm atom\,cm^{-2}\,mag^{-1}},$$

Table 1. Low-ionization 2QZ absorption systems.

2QZ QSO ID	b_J	z_{QSO}	z_{abs}	W_0[2]	Ion[1]
J095605.0−015037	19.04	1.188	1.045	3.04	efl
J095938.2−003501	19.42	1.872	1.598	4.31	fl
J101230.1−010743	19.28	2.360	1.370	2.83	fl
J101556.2−003506	18.63	2.497	1.489	2.29	cefgl
J101636.2−023422	19.55	1.519	0.912	2.90	fl
J101742.3+013216	18.35	1.457	1.313	1.72[3]	fl
J102645.2−022101	19.65	2.401	1.581	1.31[3]	cfgl
J103727.9+001819	18.48	2.466	2.301	14.0[4]	abcgijkl
J105304.0−020114	19.96	1.527	0.888	5.76	efl
J105620.0−000852	18.38	1.440	1.285	1.70	fl
J105811.9−023725	18.30	2.344	2.278	4.25[4]	acgikl
J110603.4+002207	19.06	1.659	1.018	2.08	fl
J110624.6−004923	19.84	2.414	2.122	10.3[4]	acgi
J110736.6+000328	18.86	1.726	0.953	2.65	fl
J114101.3+000825	19.89	1.573	0.841	3.93	fl
J115352.0−024609	19.42	1.835	1.204	2.90	fl
J115559.7−015420	19.05	1.259	1.132	3.75	efl
J120455.1+002640	19.23	1.557	0.597	3.92	efl
J120826.9−020531	19.35	1.724	0.761	5.31	fl
J120827.0−014524	19.69	1.552	0.621	3.13	efl
J120836.2−020727	18.42	1.081	0.873	1.97	efl
J120838.1−025712	18.70	2.327	2.314	2.44[4]	achijk
J121318.9−010203	20.14	2.515	2.415	5.33[4]	abcdgijk
J121957.7−012615	19.30	2.636	2.562	3.09[4]	acgjk
J122454.4−012753	19.63	1.347	1.089	2.14	fl
J125031.5+000216	19.61	2.100	1.327	2.61	fl
J125359.6−003227	19.48	1.689	1.503	5.44	cf
J125658.3−002123	19.05	1.273	0.947	3.62	fl
J130019.9+002641	18.81	1.748	1.225	5.92	fl
J130433.0−013916	19.56	1.596	1.410	8.05	fl
J130622.8−014541	18.98	2.152	1.332	3.67	fl
J133052.4+003219	18.73	1.474	1.327	1.89	fl
J134448.0−005257	19.52	2.083	0.932	5.44	efl
J134742.0−005831	19.32	2.515	1.795	3.69[5]	bcgikl
J135941.1−002016	18.57	1.389	1.120	2.97	fl
J140224.1+003001	19.25	2.411	1.387	2.85	fl
J140710.5−004915	19.25	1.509	1.484	3.49	fl
J141051.2+001546	18.94	2.598	1.170	4.74	efl
J141357.8+004345	20.14	2.751	2.308	5.81[4]	abcdgijkl
J142847.4−021827	18.97	1.312	1.313	2.24	fl
J144715.4−014836	19.27	1.606	1.354	2.02	fl
J214726.8−291017	19.39	1.678	0.931	1.74	fl
J214836.0−275854	18.40	1.998	1.112	1.40	fl
J215024.0−282508	19.03	2.655	1.144	1.88	efl
J215034.5−280520	18.63	1.358	1.139	1.58	fl
J215102.9−303642	19.78	2.525	2.488	7.48[4]	abcgik
J215222.9−283549	18.51	1.228	0.927	2.59	efl
J215342.9−301413	19.03	1.729	1.037	1.54	efl
J215359.0−292108	18.75	1.160	1.036	3.33	fl
J215955.4−292909	18.85	1.477	1.241	6.24	efl
J220003.0−320156	19.17	2.047	1.135	3.20	fl
J220137.0−290743	19.36	1.266	0.600	3.81	fl
J220208.5−292422	18.96	1.522	1.490	2.98	cfgl
J220214.0−293039	18.45	2.259	1.219	3.39	fl
J220650.0−315405	19.67	2.990	2.526	3.84[4]	acgk
J220655.3−313621	19.31	1.550	0.754	4.60	efl
J220738.4−291303	19.57	2.688	2.666	1.58[4]	abcik
J221155.2−272427	18.80	2.209	1.390	2.76	fl
J221445.9−312130	18.88	2.190	1.937	2.24[5]	cgk
J221546.4−273441	19.14	1.967	0.785	2.86	efl
J222849.4−304735	19.00	1.948	1.094	3.86	fl
J223309.9−310617	18.64	1.702	1.146	2.58	efl
J224009.4−311420	19.23	1.861	1.450	2.04[6]	fl
J225915.2−285458	19.07	1.986	1.405	4.57	fl
J230214.7−312139	19.71	1.699	0.955	1.98	fl
J230829.8−285651	19.06	1.291	0.726	3.94	efl
J230915.3−273509	19.20	2.823	1.060	4.66	fl
J231227.4−311814	18.70	2.743	1.555	2.95	fl
J231412.7−283645	19.31	2.047	1.920	3.18[5]	bcghikl
J231459.5−291146	18.68	1.795	1.402	3.12	fl
J231933.2−292306	19.55	2.013	1.846	4.18[5]	bcgil
J232023.2−301506	19.60	1.149	1.078	3.50	fl
J232027.1−284011	19.10	1.300	1.304	2.84	efl
J232330.4−292123	19.47	1.547	0.811	3.70	fl
J232700.2−302636	18.97	1.921	1.476	6.41	cefgil
			0.673	3.60	fl
J232914.9−301339	19.64	1.494	1.294	2.78	fl
J232942.3−302348	19.35	1.829	1.581	6.99	cfl
J233940.1−312036	19.16	2.611	1.444	2.34	fl
J234321.6−304036	18.90	1.956	1.052	2.87	fl
			1.929	0.70[5]	bcdgil
J234400.8−293224	18.26	1.514	0.851	3.13	fl
J234402.4−303601	19.62	0.844	0.852	3.75	efl
J234405.7−295533	18.55	1.705	1.359	2.88	fl
J234527.5−311843	18.30	2.065	0.828	6.67	fl
J234550.4−313612	18.89	1.649	1.138	1.95	efl
J234753.0−304508	18.56	1.659	1.421	2.49	fl
J235714.9−273659	18.92	1.732	0.814	3.52	fl
J235722.1−303513	19.36	1.910	1.309	3.65	fl
J000534.0−290308	18.90	2.353	1.168	4.83	efl
			2.226	2.59[4]	abcgik
J000811.6−310508	19.05	1.683	0.715	2.55	fl
J001123.8−292500	18.50	1.275	0.605	6.82	efl
J001233.1−292718	19.07	1.565	0.913	2.83	efl
J002832.3−271917	18.52	1.622	0.753	1.83	fl
J003142.9−292434	18.76	1.586	0.930	5.39	efl
J003533.7−291246	20.00	1.492	1.457	3.78	efl
J003843.9−301511	18.58	1.319	0.979	2.93	fl
J004406.3−302640	19.68	2.203	1.042	3.10	fl
J005628.5−290104	18.60	1.809	1.409	3.63	efl
J011102.0−284307	18.59	1.479	1.156	3.24	fl
J011720.9−295813	19.36	1.646	0.793	2.53	fl
J012012.8−301106	18.96	1.195	0.684	4.01	fl
J012315.6−293615	18.66	1.423	1.113	2.30	efl
J012526.7−313341	19.07	2.720	2.178	5.03[4]	abcdgijkl
J013032.6−285017	19.32	1.670	1.516	3.37	fl
J013356.8−292223	20.09	2.222	0.838	4.64	efl
J013659.8−294727	18.43	1.319	1.295	3.01	fl
J014729.4−272915	19.29	1.697	0.811	3.92	fl
J014844.9−302817	18.39	1.109	0.867	1.75	fl
J015550.0−283833	20.09	0.946	0.677	2.62	fl
J015553.8−302650	19.49	1.512	1.316	3.18	fl
J015647.9−283143	19.63	0.919	0.884	3.14	fl
J015929.7−310619	18.98	1.275	1.079	1.56	fl
J021134.8−293751	18.97	0.786	0.616	3.45	efl
J021826.9−292121	19.20	2.469	1.205	4.45	efl
J022215.6−273231	19.20	1.724	0.611	2.55	efl
J022620.4−285751	18.43	2.171	1.022	9.03	efl
J023212.9−291450	19.67	1.835	1.212	4.63	fl
			1.287	3.06	fl
J024824.4−310944	18.59	1.399	0.789	4.91	efl
			1.371	1.37	efl
J025259.6−321125	18.78	1.954	1.735	3.94[3]	cfghkl
J025607.9−311732	18.78	1.255	0.903	3.78	efl
			0.975	4.62	efl
J025919.2−321650	19.34	1.557	1.356	3.15	fl
J030249.6−321600	18.27	0.898	0.821	4.54	fl
J030324.3−300734	18.69	1.713	1.190	2.95	fl
J030647.6−302021	19.03	0.806	0.745	4.21	fl
J030711.4−303935	19.09	1.181	0.966	2.81	efl
			1.108	2.79	efl
J030718.5−302517	19.48	0.992	0.711	4.95	efl
J030944.7−285513	19.35	2.117	0.931	3.39	fl
J031255.0−281020	19.21	0.954	0.953	2.06	fl
J031309.2−280807	19.15	1.435	0.950	1.78	fl
J031426.9−301133	18.41	2.071	1.128	6.08	efl
			1.631	1.20[3]	fl

[1] Ion identifications: a, H I; b, C II; c, C IV; d, O I; e, Mg I; f, Mg II; g, Al II; h, Al III; i, Si II; j, Si III; k, Si IV; l, Fe II.
[2] Rest equivalent width of Mg II λλ2796,2803 doublet (Å) unless stated explicitly below.
[3] Rest equivalent width of Fe II λ2600 (Å) (Mg II blended with sky line).
[4] Rest equivalent width of H I λ1215 (Å).
[5] Rest equivalent width of C IV λλ1548,1550 doublet (Å).
[6] Rest equivalent width of Mg II λ2796 (Å) only.

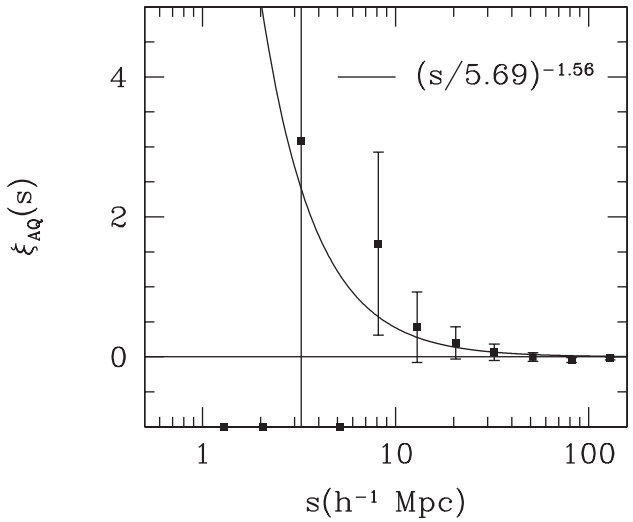

Figure 2. The two-point cross-correlation function between the QSO absorbers and 2QZ QSOs, $\xi_{AQ}(s)$, calculated in an $\Omega_m = 0.3$, $\Omega_\Lambda = 0.7$ cosmology. Overlaid is the best-fitting power law to the QSO autocorrelation function measured by Croom et al. (2001b).

we obtain an average neutral hydrogen column of $N(\mathrm{H\,I}) \sim 2.3 \times 10^{20}$ atom cm^{-2} for our absorbers. This is approximately the minimum column density of a DLA, and is probably considerably smaller than the average neutral hydrogen column of our sample. The reason for this is that the dust-to-gas ratio in high redshift DLAs is typically much lower than in the local interstellar medium. Using zinc and chromium abundance measurements, Pettini et al. (1997) found that the average dust-to-gas ratio in DLAs at $\bar{z} \sim 2.5$ is $\sim$ 1/30 of that in the Milky Way. Our sample of absorbers is at a lower redshift and, assuming an average neutral hydrogen column of $N(\mathrm{H\,I}) \sim 10^{21}$ atom cm^{-2}, the observed extinction appears consistent with a dust-to-gas ratio of about one-quarter that of the Milky Way. It is possible that selection effects could bias our sample towards higher metallicity or column density. Further observations could be used to determine these quantities, and hence allow a more reliable measurement of the dust in these systems.

ACKNOWLEDGMENTS

The 2QZ is based on observations made with the Anglo-Australian Telescope and the UKST, and we would like to thank our colleagues on the 2dF galaxy redshift survey team and all the staff at the AAT that have helped to make this survey possible. NSL acknowledges the receipt of a PPARC studentship.

REFERENCES

Bailey J. A., Glazebrook K., 1999, 2dF User Manual. Anglo-Australian Observatory
Bohlin R. C., Savage B. D., Drake J. F., 1978, ApJ, 224, 132
Croom S. M., Shanks T., 1999, MNRAS, 303, 411
Croom S. M., Smith R. J., Boyle B. J., Shanks T., Loaring N. S., Miller L., Lewis I. J., 2001a, MNRAS, 322, L29
Croom S. M., Shanks T., Boyle B. J., Smith R. J., Miller L., Loaring N. S., Hoyle F., 2001b, MNRAS, 325, 483
Fan X. et al., 1999, AJ, 118, 1
Lanzetta K. M., Wolfe A. M., Turnshek D. A., 1995, ApJS, 440, 435
Le Brun V., Bergeron J., Boissé P., Deharveng J. M., 1997, A&A, 321, 733
Lewis I. J., Glazebrook K., Taylor K., 1998, Proc. SPIE, 3355, 828
Mo H. J., Mao S., White S. D. M., 1999, MNRAS, 304, 175
Pei Y. C., Fall S. M., 1995, ApJ, 454, 69
Pettini M., King D. L., Smith L. J., Hunstead R. W., 1997, ApJ, 478, 536
Pettini M., Ellison S. L., Steidel C. C., Bowen D. V., 1999, ApJ, 510, 576
Rao S. M., Briggs F., 1993, ApJ, 419, 515
Rao S. M., Turnshek D. A., 1998, ApJ, 500, L115
Schlegel D. J., Finkbeiner D. P., Davis M., 1998, ApJ, 500, 525
Smith R. J., Boyle B. J., Maddox S. J., 1995, MNRAS, 277, 270
Smith R. J., Croom S. M., Boyle B. J., Shanks T., Miller L., Loaring N. S., 2001, MNRAS, submitted
Vladilo G., 1999, in Mahoney T. J., Beckman J. E., eds, ASP Conf. Ser., The Evolution of Galaxies on Cosmological Timescales. Astron. Soc. Pac., San Francisco (astro-ph/9903406)
Wolfe A. M., 1995, in Meylan G., ed., QSO Absorption Lines. Springer, Berlin, p. 13

This paper has been typeset from a TEX/LATEX file prepared by the author.